This is the accepted manuscript made available via CHORUS. The article has been published as:

Separating β relaxation from α relaxation in fragile metallic glasses based on ultrafast flash differential scanning calorimetry

M. Gao and J. H. Perepezko

Phys. Rev. Materials **4**, 025602 — Published 20 February 2020

DOI: 10.1103/PhysRevMaterials.4.025602

Separating β relaxation from α relaxation in fragile metallic glasses based on ultrafast Flash DSC

M. Gao, J. H. Perepezko*

University of Wisconsin- Madison, Department of Materials Science and Engineering, Madison, WI 53706

*Corresponding author. Tel.: +1 6082631678. E-mails: perepezk@engr.wisc.edu (Prof. J. H. Perepezko).

ABSTRACT

Despite numerous studies on the glass transition and the related relaxation dynamics, the physical mechanism of activation of multiscale relaxation events under various external stimuli in amorphous materials is still unclear. In this study, by combining the traditional DSC and Flash DSC with heating rates spanning over five orders of magnitude, the thermodynamic responses have been systematically studied for several fragile and strong metallic glasses. A common endothermic event before the glass transition is detected when the heating rate increases above a critical value for fragile metallic glasses. This endothermic event is verified to represent the activation of secondary β relaxation (Johari-Goldstein relaxation), which is commonly found in amorphous materials. For fragile metallic glasses, with the increase of fragility, the critical heating rate to separate the β relaxation from the α relaxation decreases. In contrast, the β relaxation does not appear within the current experimental heating rate limit for strong glass systems. Finally, based on the potential energy landscape model and the flow unit model of the heterogeneous structure for MGs, a pathway is proposed for the fragile and strong MGs to understand the physical mechanism for the separation of the β relaxation from the α relaxation via ultrafast heating. This study clearly demonstrates that the Flash DSC with wide heating rate range is an effective tool to study the relaxation dynamics in amorphous materials.

Key words: α and β relaxation, ultrafast heating, fragility, heterogeneity, metallic glasses

I. INTRODUCTION

For various amorphous materials, one of the typical characteristics of the glass transition is the slowing down of the main relaxation process (named as α relaxation) when the temperature gradually decreases into the glass transition temperature [1-5]. According to the relaxation spectrum for amorphous materials, except for the dominant α relaxation corresponding to the glass transition, a secondary relaxation event, commonly called the Johari-Goldstein or β relaxation, often appears at higher frequencies below the glass transition temperature [2]. Moreover, different amorphous materials exhibit different relaxation spectra. For example, for molecular glasses, several distinct relaxation peaks, such as the primary (α) peak, the secondary (β) peak and even the third (γ) peak have been observed [6-7]. By comparison, for metallic glasses (MGs) with disordered structure and simple metallic bonding, it was initially thought that there could be only one primary relaxation peak (α relaxation) on the relaxation spectrum [8-9]. However, there are many recent reports indicating that MGs could also exhibit the secondary β relaxation under dynamic mechanical stimulus [10-16]. It has been found that the secondary β relaxation is closely related to the macroscopic tensile ductility [13], the diffusion motion of small atoms within an amorphous structure [14], the activation of the shear-transformation-zones (STZs) and the intrinsic heterogeneities in MGs [15-16]. In view of the fundamental importance and the technological relevance, the discovery of the β relaxation in MGs has triggered a great deal of research interest [13-16, 17-18]. However, there is still much unknown about the secondary β relaxation in MGs, such as the activation process of the secondary β relaxation under different external stimuli for various MGs with different fragilities.

There have been a large number of experimental results indicating that the MGs are not completely homogeneous at the nanoscale and there exist structural heterogeneities that have been identified as flow units (also termed as liquid-like zones or weakly bonded regions) [19-21]. These structural heterogeneities show a low modulus, a low viscosity and a high atomic mobility. Thus, the structure of MGs can be considered as a random distribution of flow units embedded in an elastic matrix [16]. Then, based on the above heterogeneous flow unit model for MGs, the secondary β relaxation in MGs corresponds to the activation of flow unit regions [16, 18]. On the other hand, according to the relaxation activation spectrum within the external stimuli frequency domain, the secondary β relaxation can be activated by higher frequency stimuli in contrast to the occurrence of a distinct α relaxation in the low frequency range [22].

Thus, considering the difference in the dynamic properties (such as the local elastic modulus, viscosity and atomic mobility) and the activation frequency of the α relaxation and β relaxation, the primary α relaxation and secondary β relaxation should be separated by tuning the dynamic external stimuli frequency range. Two commonly used external stimuli are the load and the temperature. Previous studies of the β relaxation in MGs were mainly based upon the dynamic mechanical analysis method (DMA) [10-16, 22-23]. For the DMA methods, the external stimuli are the dynamic stress or strain and the primary α relaxation and secondary β relaxation separately appear in different frequency domains. 15 In contrast, only a few studies have focused on the calorimetric study of secondary β relaxation by modulated differential scanning calorimetry (MDSC) together with annealing treatments [24-27]. Considering that the measurement range of heating rate for conventional DSC is extremely limited (just several K/s), only the primary α relaxation appears in the heat flow curve during heating and the thermodynamic behaviors at higher heating rates are still unknown. Recently, one advanced commercial chip-based fast differential scanning calorimeter (Mettler Toledo Flash DSC 1) enables thermo-analytical measurements at orders of magnitude higher rates and the maximum heating and cooling rate can reach 4×10^4 K/s and 1×10^4 K/s, respectively [28-29]. Meanwhile, considering that various relaxation events in amorphous materials should have different unique dynamic properties and have their own evolution paths, additional relaxation events can be separated within the large heating rate range covering over 4 orders of magnitude in Flash DSC platform. For the thermal activation processes, such as the crystallization and the glass transition, it has been verified that the relationship between the typical temperature (crystallization temperature or glass transition temperature) and the heating rate for MGs can be roughly described by the Kissinger equation or Arrhenius equation [30-37]. Based on this hypothesis, the primary crystallization and glass transition in marginal Al-based MGs without the glass transition signal can be easily separated by the advanced Flash DSC, which is not available for traditional thermal analysis methods [38-40]. Therefore, it is of special interest to determine if the secondary β relaxation event can be separated from primary α relaxation within large heating rate range for MGs.

In this work, we show that the primary α relaxation and the secondary β relaxation in a series of fragile MG systems can be separated by Flash DSC with fast heating rates. For a typical fragile Pd-based MG, a distinct endothermic peak before the glass transition temperature is

detected by Flash DSC, which is verified as the β relaxation. Then, the relaxation time and effective relaxation activation energy for α relaxation and β relaxation were obtained within a large heating rate range covering over 4 orders of magnitude, and clearly show the separation of the α relaxation and the β relaxation under larger heating rates. Secondly, the thermal responses under ultrafast heating for other fragile MG systems were examined and a similar endothermic peak before the glass transition temperature was detected when the heating rate increases above a critical value. For MGs with increasing fragility, the critical heating rate to separate the β relaxation from the α relaxation decreases. In contrast, only the main α relaxation is observed for the strong MG systems. Finally, a physical mechanism based on the flow unit model and potential energy landscape model is proposed to understand the difference in the separation of the β relaxation from the α relaxation for fragile and strong MG systems by ultrafast heating.

II. EXPERIMENTAL METHODS

Seven MG systems with markedly different kinetic properties (usually characterized by the kinetic fragility, m) were selected for the experiments. The compositions of these MG systems are $Pd_{40}Ni_{10}Cu_{30}P_{20}$, $Mg_{65}Cu_{25}Gd_{10}$, $Au_{49}Cu_{26.9}Ag_{5.5}Pd_{2.3}Si_{16.3}$, $La_{60}Ni_{15}Al_{25}$, $Zr_{41.2}Ti_{13.8}Cu_{12.5}Ni_{10}Be_{22.5}$, $Gd_{55}Co_{25}Al_{20}$ and $Al_{88}Y_7Fe_5$. For the Pd-, Au-, La-, Zr-, Gd- and Al-based MGs, the ingots were prepared by arc melting and the elemental components were melted for several times in a Ti-gettered argon atmosphere to ensure the homogeneity. For the Mg-based MG, the ingot was prepared by an induction melting method in an argon atmosphere. Then, the ribbon samples for the above compositions were prepared by single-roller melt spinning on a copper wheel with the tangential speed of 55 m/s. The ribbons have a cross section about 2 mm×20 μm and about several meters in length. The cooling rates for preparing the ribbon-like samples in this work can be estimated as about 2.5×10^6 K/s (See Supplementary Material [41] and the method is described in Ref. [42]). The glassy nature for all ribbon-like samples was ascertained by X-ray diffraction (Bruker D8 Discover Diffraction with Cu K_α radiation) and differential scanning calorimetry (PerkinElmer Diamond DSC). The samples for all the DSC tests including the conventional DSC, step-scan DSC and Flash DSC tests are from the above as-cast ribbons and the as-cast ribbons are cut into different sizes to be suitable for different DSC instruments.

A high-rate differential scanning calorimeter with chip sensors (Flash DSC 1, the maximum heating rate and cooling rate are 4×10^4 and 1×10^4 K/s respectively, Mettler Toledo) was used to investigate the thermal behaviors of various MGs systems under different heating rates from 5 K/s to 10000 K/s. The measurement temperature range for Flash DSC 1 is between -90 ^{o}C and 450 ^{o}C. The as-cast ribbon-like samples were cut into tiny pieces of approximately 150 μm×150 μm× 20 μm (length×width×thickness) and then were loaded onto the Flash DSC chip. As a reference, the heat flow curves with low heating rates from 0.17 K/s to 3.3 K/s were also measured by Diamond DSC. For conventional DSC tests, the as-cast ribbon-like samples are cut into small pieces by a scissor and the dimensions of each piece are about 5 mm×2 mm× 20 μm (length×width×thickness), which is suitable to be loaded into the aluminum pan for conventional DSC measurements. Considering the tiny sample for Flash DSC measurements and the related the mass effect [28-29], we prepared two other Pd-based samples with sizes of about 100 μm and 50 μm to demonstrate that the mass effect can be neglected (See Fig. S1 [41] and the density can be seen Ref. [43]). The conventional DSC and Flash DSC instruments have been calibrated before testing and the detailed calibration methods are given in Fig. S2 [41] and Ref. [44].

To verify that the first endothermic reaction observed by Flash DSC before the glass transition temperature corresponds to the activation of the secondary β relaxation event for the Pd-based MG, the heat capacity curve with temperature was measured by the step-scan mode (temperature modulated DSC technique) in the Perkin-Elmer Diamond DSC to reveal the multiscale relaxation signals [45]. The step-scan method consists of multiple temperature ramp/isothermal steps. The step sizes were 2 K, the holds were 1 min at each temperature, and a 0.33 K/s (20 K/min) heating or cooling rate was used between sequential isothermal hold temperatures. Measurements were performed in the temperature range from 283 to 673 K. The heat capacity c_p at one temperature was then established by using the measured heat release at each heating step [45]. The sample size for the step-scan test is the same with the above conventional DSC tests and the dimensions of each piece are about 5 mm×2 mm× 20 μm (length×width×thickness).

III. RESULTS AND DISCUSSIONS

A. Thermal responses with different heating rates in Pd-based MG

A typical Flash DSC heat flow curve with heating rate of 1000 K/s from 350 K to 673 K for the as-cast fragile Pd-based MG is shown in the Fig. 1. The inserted optical images give the sample exterior morphology transformation from square-like to spherical-like before and after heating on

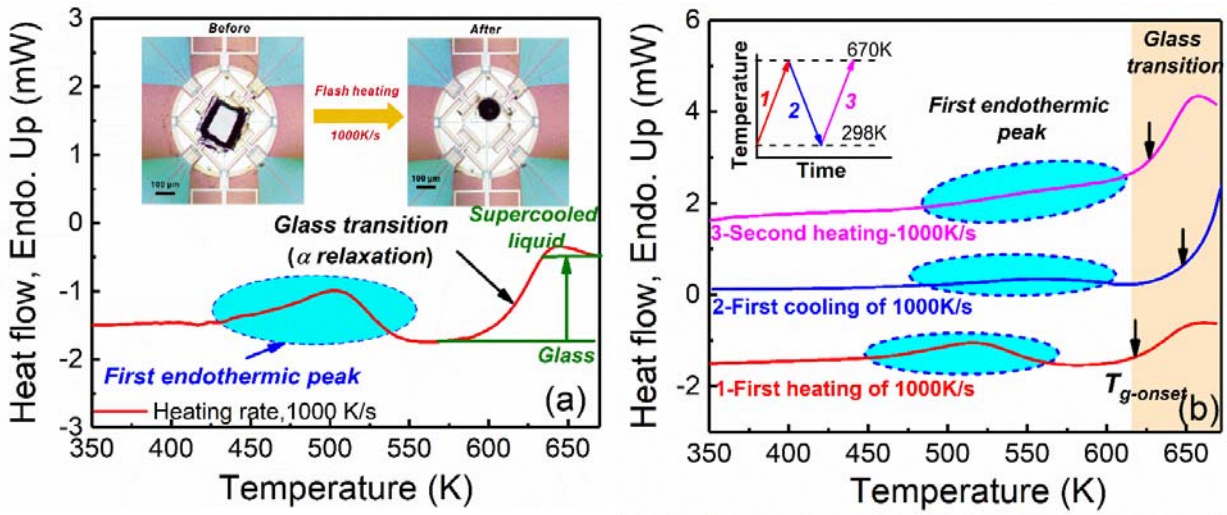

FIG. 1. (a) A typical Flash DSC heat flow curve at the heating rate of 1000 K/s for the as-cast Pd-based MG sample. The inserted optical pictures give the transformation process for the surface morphology of the tiny sample before (square-like) and after (spherical-like) heating on the chip sensor. (b) Comparison of heat flow curves based on the inserted temperature program. The temperature program includes two heating stage and one cooling rate stage and the heating rate and cooling rate are 1000 K/s.

the chip sensor. It is evident that the tiny Flash DSC sample exhibits a shape change induced by the transition from the glass state to supercooled liquid state during ultrafast heating, but maintains contact with the chip sensor. Moreover, it is interesting to find that there appear two significant endothermic events during Flash DSC heating in Fig. 1, which is different from the heat flow curves by conventional DSC on the Pd-based MG (Seen in Fig. 2(a)). The peak value of the second endothermic event at about 643 K is actually the glass transition signal considering the step difference of heat capacity between the glass state and supercooled liquid state in Fig. 1 [46]. However, below the glass transition temperature, there exists another obvious endothermic peak at about 505 K with no obvious step difference of heat capacity before and after the first

endothermic reaction, which is not the typical thermal signal for the glass transition. This distinct first endothermic peak before the glass transition temperature is directly detected by the thermal scanning method in the Pd- based MG. For the glass transition (α relaxation), the process is usually reversible during cooling and heating except for the thermal hysteresis [2-5]. For the observed first endothermic reaction before glass transition, the temperature program in the insertion of Fig. 1(b) was also applied to test if the first endothermic reaction is reversible (one new Flash DSC sample from the same Pd-based amorphous ribbon was used). One can clearly see that the heat flow curve for the first cooling with cooling rate of 1000 K/s after first heating (the first cooling rate is the same with the first heating rate) also shows the first endothermic peak before glass transition temperature, which is similar with the first endothermic peak in Fig. 1(a). The difference for the first heating and first cooling heat flow curves is that the peak values of glass transition and the first endothermic reaction for the first cooling stage shift to the higher temperatures compared to the first heating flow stage. There also exists a thermal hysteresis of the first endothermic reaction for the heating and cooling with the same rate of 1000 K/s. Moreover, when the sample was heated again with the same heating rate of 1000 K/s, there also appears the first endothermic peak and the peak values of glass transition and the first endothermic reaction shift to the high temperature range compared to the first heating stage. For the first heating stage, the sample was as-cast and the cooling rate for the as-cast sample is about 2.5×10^6 K/s, which is much larger than that of the second heating stage. Thus, the sample with cooling rate of 1000 K/s for the second heating stage can be considered as an annealed sample compared to the as-cast sample with the cooling rate of 2.5×10^6 K/s. From the perspective of the effective structural relaxation effect, the increase of the peak value of glass transition for the sample during the second heating stage is reasonable.

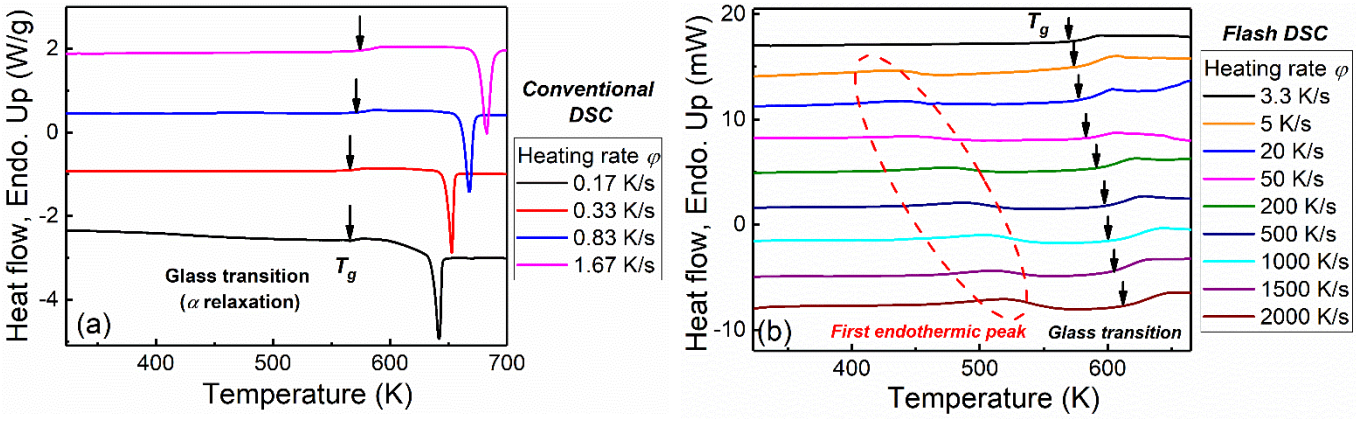

FIG. 2. (a) A series of heat flow curves at the heating rates from 0.17 K/s to 1.67 K/s by conventional DSC for Pd-based MG samples. (b) A series of heat flow curves at the heating rates from 3.3 K/s to 2000 K/s by Flash DSC for Pd-based MG samples. The downward black arrows point the onset temperature of the glass transition. The red dashed curve marks the appearance of the first endothermal reaction before the glass transition.

To investigate the kinetic evolution behaviors of the first endothermic reaction in the Pd-based MG, a series of heat flow curves with different heating rates from 3.3 K/s to 2000 K/s were measured by Flash DSC in Fig. 2(b). For each test corresponding to one different heating rate, one new tiny flash DSC sample from the same amorphous ribbon was replaced. As a reference, the heat flow curves by conventional DSC with different heating rates from 0.17 K/s to 1.67 K/s were also obtained in Fig. 2(a). It is evident that there only appears one endothermic event corresponding to the glass transition in all conventional DSC heat flow curves. In contrast, when the heating rate increases above about 5 K/s during a Flash DSC run, a new endothermic peak appears before the corresponding glass transition temperature. This indicates that the first endothermic reaction only takes place when the heating rate increases above a critical value. Moreover, with the increase of heating rate, both the values for the first endothermic peak temperature and glass transition peak temperature shift the higher temperatures, which suggests that the first endothermic reaction and glass transition can be roughly considered as thermally activated processes and the effective activation energy for both can be obtained by fitting the Kissinger equation [30]. Thus, based on the results in Fig. 2, the Kissinger plots [30]. for the first endothermic reaction and glass transition are presented in Fig. 3(a). It is evident that for the first endothermic reaction the Kissinger equation can fit the experimental results very well. In contrast, for glass transition the Kissinger plot at a low heating rate range exhibited as a straight line, but a curvature develops when the heating rate increases above about 200 K/s as indicated in Fig.3. From the previous research, the glass transition cannot be considered as a simple thermal activation process, especially in the high temperature range [5, 31-32, 40]. On the other hand, the Kissinger plots with limited heating rate range usually exhibit as straight lines, giving a constant activation energy within a small temperature range [32]. Thus, by fitting the experimental data with the Kissinger equation, $\ln(\frac{\varphi}{T_{peak}^{2}}) = C + \frac{Q}{R}\frac{1}{T_{peak}}$ (φ is the heating rate, R is the gas constant, Q is the effective activation energy and C is a constant), the effective

activation energies can be obtained for the first endothermic reaction and the glass transition. From Fig. 3(a), the values of the activation energy for the first endothermic reaction and the glass transition are 97±4 kJ/mol and426±13 kJ/mol, respectively. It is noted that the value of effective activation energy for the glass transition is much larger than that of the first endothermic reaction, which implies that the dynamic evolution behaviors for the first endothermic reaction and glass transition are significantly different. These results about the first endothermic reaction

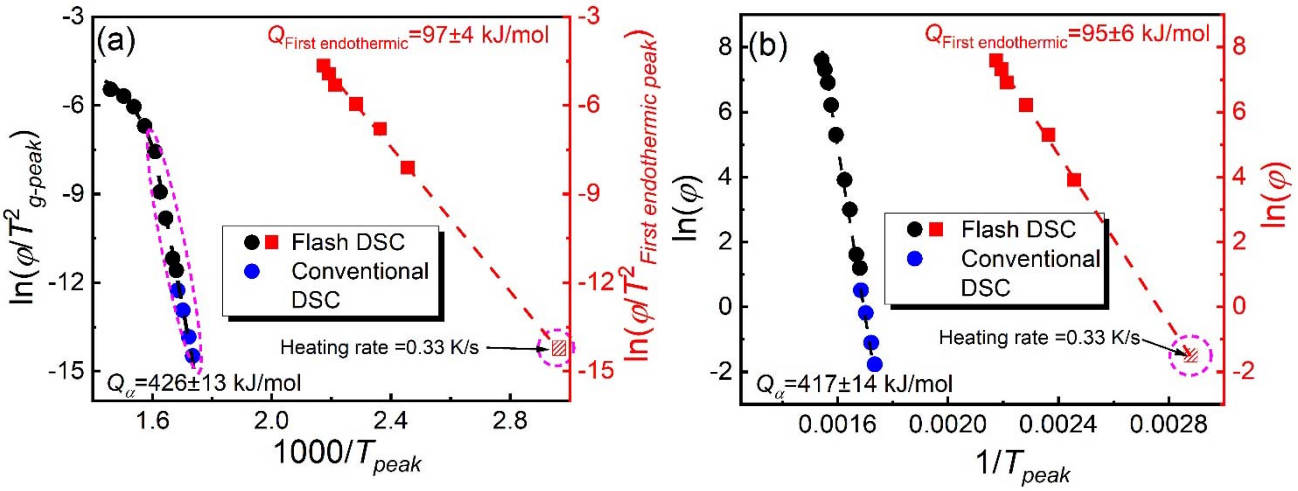

FIG. 3. (a) Activation energies for the first endothermic reaction and the glass transition by fitting the Kissinger equation of $\ln\left(\frac{\varphi}{T^2}\right) = A - \frac{Q}{R}\left(\frac{1}{T}\right)$ (A is a constant and R is the gas constant) based on the heat flow curves in FIG. 2(a) and 2(b). (b) Activation energies for the first endothermic reaction and the glass transition by fitting the Arrhenius equation of $\ln(\varphi) = B - \frac{Q}{R}\left(\frac{1}{T}\right)$ (B is a constant) based on the heat flow curves in FIG. 2(a) and 2(b). The extrapolated points in FIG. 3(a) and 3(b) are marked by magenta dashed circles.

are similar to those for the endothermic β relaxation signal for MGs that can be detected by temperature modulated DSC method based on the isothermal treatments [33, 47]. Based on the previous studies, the values of activation energy Q_β for thermal β relaxations were reported to be much smaller than those of the corresponding glass transition signals. Moreover, there exists an approximately linear relationship between Q_β and T_g given by Q_β= (26±2)RT_g [47]. In the current work, it is noteworthy to find that the values of $Q_{First\ endothermic}$ and T_g are 97±4 KJ/mol and 560 K and $Q_{First\ endothermic}$≈(21±1)RT_g. The reversible nature of the first endothermic reaction and the

linear relationship between the Q_β and T_g are consistent with the previous results about the thermal β relaxation [26, 47]. Moreover, since the sample can be readily removed from the chip after testing the possibility that the endothermic signal before glass transition originates from mechanical interactions between the chip and film can be excluded. In addition, any recovery signal from the release of stored strain energy in the sample is expected to be exothermic as is well documented for crystalline materials.

Meanwhile, it should be noted that while the response of both the peak values of the glass transition and the first endothermic reaction-β relaxation to the increases in heating rate is similar to the response of thermally activated reactions, the representation of the temperature and heating rate dependence has been presented differently in the literature [14, 33-37]. For example, the dependence of glass transition temperature T_g and β relaxation on heating rate has been represented by the Kissinger equation, but this equation was derived for a first order transformation such as crystallization [14, 34-36]. However, Ruitenberg has presented an analysis justifying the use of the Kissinger equation for the heating rate dependence of T_g and the interpretation of the effective activation energy [37]. Alternatively, the heating rate dependence of T_g has been reported to follow a simple Arrhenius equation and also to be related to the viscosity behaviors, which have yielded different functional forms of T_g and heating rate considering different factors [31-32, 40]. In fact, the values of the effective activation energy for glass transition by Kissinger equation and Arrhenius equation within the small temperature range are very close [37]. Here, we also calculated the effective activation energy for β relaxation and glass transition by fitting the Arrhenius equation and the values of $Q_{\beta\text{-}Arrhenius}$ and $Q_{\alpha\text{-}Arrhenius}$ are 417±14 and 95±4 kJ/mol in Fig. 3(b), which are close to those by fitting the Kissinger equation in Fig. 3(a). Separately, in the analysis of DMA results, the frequency response has been analyzed in terms of an Arrhenius equation [15]. Thus, considering that each of the reported analysis methods has some merit in order to compare the heating rate dependence of T_g and the β relaxation, we used both of the Kissinger equation and the Arrhenius equation as a common basis to study the evolution of T_g and the β relaxation with heating rates.

To further verify if the first endothermic reaction before glass transition is the thermal β relaxation, the step-scanning DSC method was applied to measure the heat capacity curve with temperature [48-49]. The detailed temperature program is presented in Fig. 4(a). Based on the

previous studies on the thermal β relaxation, the multiscale relaxation signals can be identified in the heat capacity curve [48-49]. As shown in Fig. 3(b), the heat capacity curve with temperature can be obtained based on the step-scanning heat flow curve. From Fig. 4, it is clear that the thermal β relaxation signal appears before the glass transition and the values of the peak temperature for the β relaxation and the peak temperature for the glass transition (α relaxation) are 337 K and 603 K, respectively. Due to the heating rate dependence of the first endothermic reaction and glass transition, the peak temperature of the first endothermic reaction and the peak temperature of the

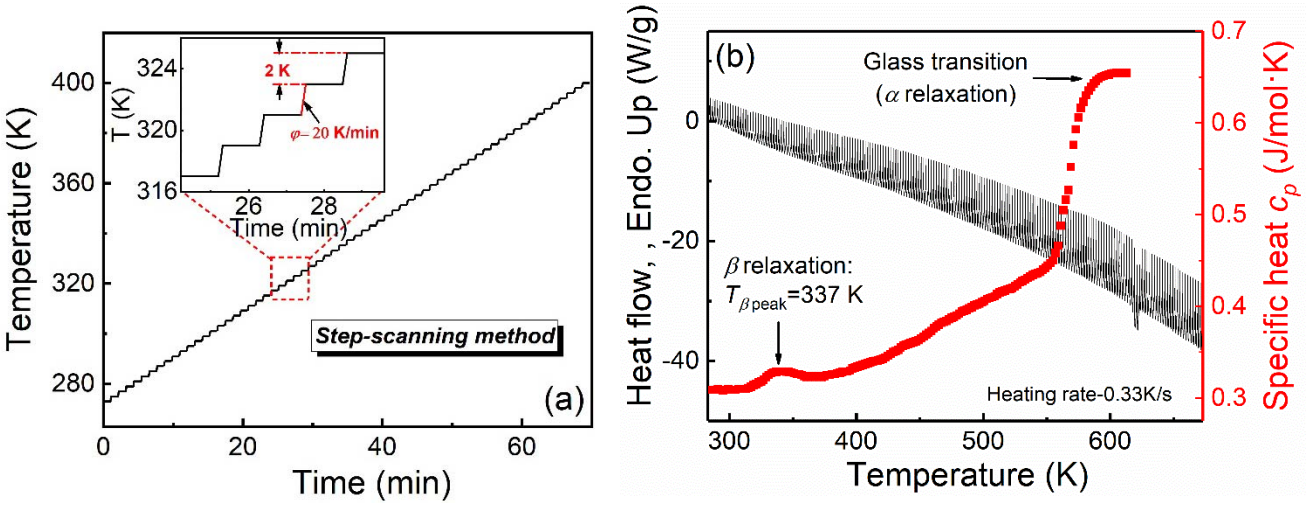

FIG. 4. (a) Temperature program for step-scanning DSC method. (b) Step-scanning heat flow curves and the corresponding heat capacity curve with temperature.

glass transition can be estimated at the heating rate of 0.33 K/s by extrapolating the Kissinger equation shown in Fig. 3(a), and the values are 340 K and 601 K, respectively. The conventional DSC measurement of T_g is about 600 K, which agrees with the above results. It is evident that the peak values for the thermal β relaxation and the first endothermic reaction are close, which further confirms that the observed endothermic reaction in Fig. 1 and Fig. 2(b) is actually the thermal β relaxation. For MGs, the thermal β relaxation usually appears in the lower temperature range compared with glass transition temperature and are considered as a string of atoms that moves back and forth reversibly and cooperatively within the confinement provided by the surrounding elastic matrix [12, 14]. Under the conventional DSC with low heating rates, the

thermal signal for the β relaxation is very weak compared to the following strong glass transition signal (Fig. 2(a)), which is induced by the e□ect of the decrease in the enthalpy by the structural relaxation during slow heating. In comparison, the Flash DSC with much higher heating rates allows the weak β relaxation to stand out and it is possible to directly detect the corresponding thermal signal for the thermal β relaxation. This principle of separating the β relaxation from the glass transition (two different dynamic processes) in this work is very similar to the previous researches of separating the weak glass transition signal from the strong primary crystallization in marginal Al-based MGs without an obvious glass transition signal during conventional DSC measurements with limited heating rating range [38-40]. Thus, the above results and analyses indicate that the secondary β relaxation for MGs can be separated from glass transition (α relaxation) when the heating rate increases above a critical value.

Moreover, it should be noted that this new method to detect the secondary β relaxation by ultrafast heating is significantly different from previous studies based on the temperature modulated method combining with the isothermal treatments [33, 47]. The external isothermal treatment usually induces a large change in the microscopic structure and the dynamic properties and the intrinsic dynamic relaxation behaviors for various MG systems cannot be obtained. The structural relaxation effect on the relaxation behaviors of MGs via Flash DSC will be the focus of future research.

B. Separation of α and β relaxation in other fragile MGs

For glass systems, the relaxation behaviors are closely related to the kinetic fragility [10, 50-51]. In addition, the rheologic behaviors of different glass formers as the temperature approaches the glass transition usually follow different patterns. The rheologic patterns during the slowing-down process can be well characterized by the "fragility", proposed by Angell, to describe different scaling behaviors of supercooled liquids with respect to temperature: $m = \left.\frac{d \log \eta}{d(T_g / T)}\right|_{T=T_g}$, where m is the fragility parameter and η is the viscosity [4-5]. For fragile liquids with a high m value, the viscosity displays a strongly non-Arrhenius dependence on temperature; in contrast strong liquids display an Arrhenius-like viscosity dependence with temperature. Meanwhile,

based on the potential energy landscape model, compared to the strong glass formers, the fragile glass formers have a higher density of configuration states, a larger degeneracy leading to rapid thermal excitation, a higher heat capacity and larger number of dynamic heterogeneities [5, 52]. Thus, fragile glasses should exhibit faster and more complex dynamic relaxation behaviors under external stimulus than strong glasses [10, 21]. From this viewpoint, the β relaxation in fragile glass formers is more sensitive to the external stimuli than that of strong glass formers. Moreover, under ultrafast heating, the β relaxation events for various fragile MGs should be more easily separated from the primary α relaxation compared to the strong MGs. In order to examine this expectation, four fragile MG formers were selected with different kinetic characters (different fragility m

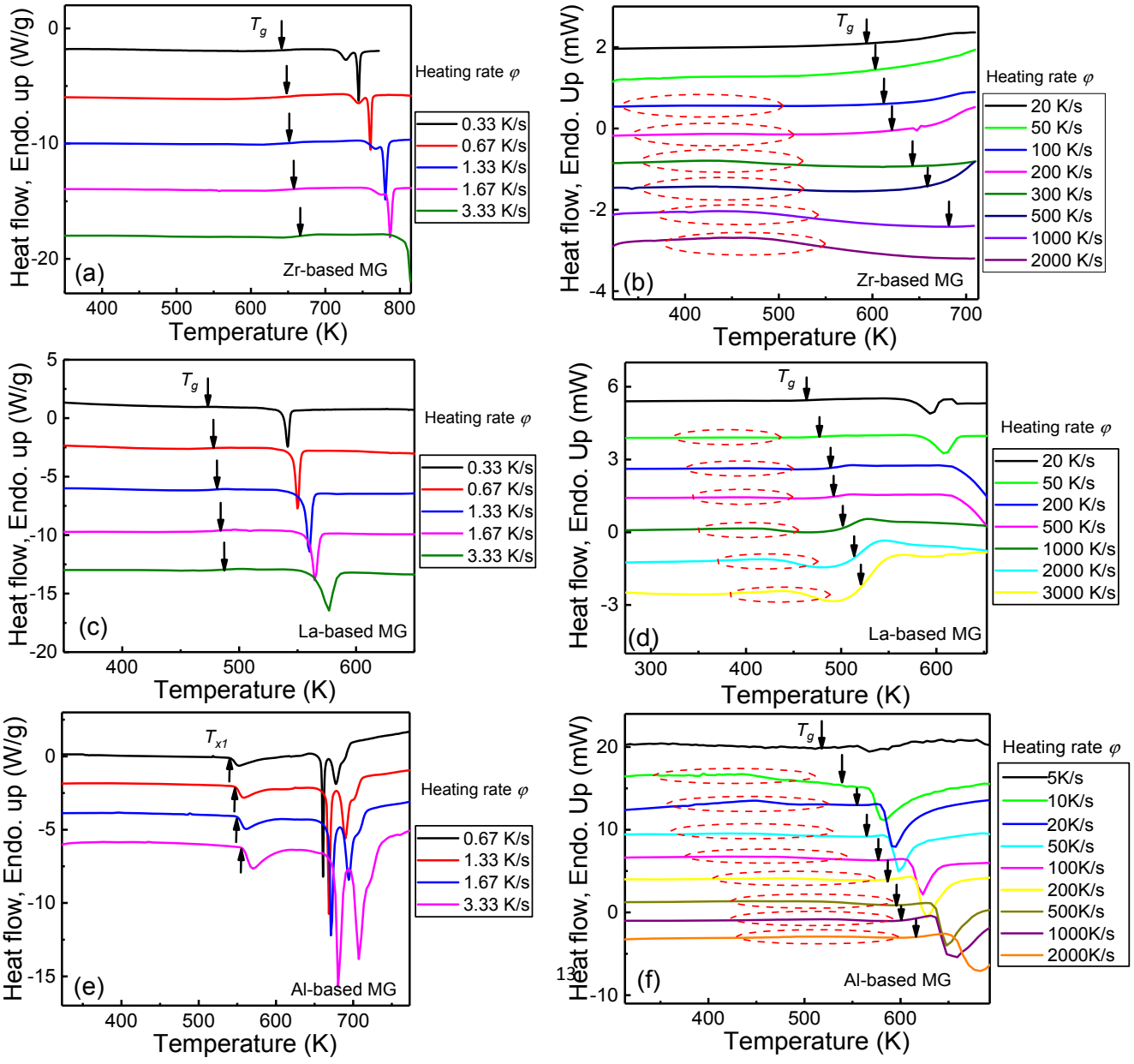

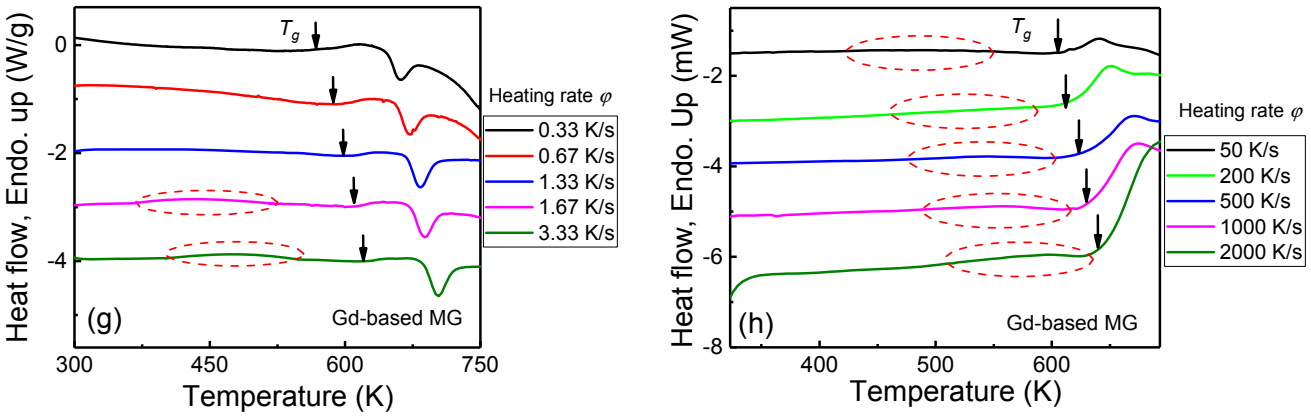

FIG. 5. (a)-(b) A series of heat flow curves with different heating rates by conventional DSC and Flash DSC for $Zr_{41.2}Ti_{13.8}Cu_{12.5}Ni_{10}Be_{22.5}$. (c)-(d) A series of heat flow curves with different heating rates by conventional DSC and Flash DSC for $La_{60}Ni_{15}Al_{25}$. (e)-(f) A series of heat flow curves with different heating rates by conventional DSC and Flash DSC for $Al_{88}Y_7Fe_5$. (g)-(h) A series of heat flow curves with different heating rates by conventional DSC and Flash DSC for $Gd_{55}Co_{25}Al_{20}$.

values): $Zr_{41.2}Ti_{13.8}Cu_{12.5}Ni_{10}Be_{22.5}$ (m=50), $La_{60}Ni_{15}Al_{25}$ (m=51), $Al_{88}Y_7Fe_5$ (m=55) and $Gd_{55}Co_{25}Al_{20}$ (m=74). For the Zr-, Pd- and Gd- based systems, the values of fragility were from Ref. [53-55]; for the Al- and La-based systems, the values of fragility were calculated based on the calorimetric measurements (see Fig. S3 [41] and Ref. [56-58]). The other physical properties for these MG systems are also listed in Table 1. A series of conventional DSC and Flash DSC runs with different heating rates from 0.33 K/s to 6000 K/s were conducted on these systems and the detailed heat flow curves are shown in Fig. 5. Again, it is apparent that there appears the first endothermic reaction (β relaxation) before the glass transition when the heating rate increases above a critical value for all fragile MG systems. For the weak fragile MG systems (smaller fragility m values), such as Zr-, La- and Al-based MG systems, the DSC heat flow curves do not show the obvious β relaxation peak in Fig. 5(a), 5(c) and 5(e) and the β relaxation signals only appear in the Flash DSC heat flow curves in Fig. 5(b), 5(d) and 5(f). In contrast, for the Gd-based MG (larger fragility m value), under the heating rate of 1.67 K/s by conventional DSC,

there appears the first endothermic reaction of β relaxation in Fig. 5(g). Based on the above heat flow curves for the different fragile MG systems, the values of critical heating rate φ_c to activate the β relaxations were determined and are listed in Table 1. The corresponding plot of fragility m and critical heating rate φ_c for all fragile MG systems is shown in Fig. 6. It is evident that the larger the m value for the MG systems, the smaller of critical heating rate to activate the β relaxation, which is consistent with the potential energy landscape model [5, 52]. Moreover, this result indicates that Based on the heat flow curves in Fig. 5, the effective activation energies for the β relaxation and the glass transition for all fragile MG systems were also calculated by fitting the Kissinger equation and the Arrhenius equation (the detailed calculations are shown in Fig. S4 [41]). First, for these fragile MGs, the Kissinger plots and the Arrhenius plots exhibit the relaxation behaviors can be

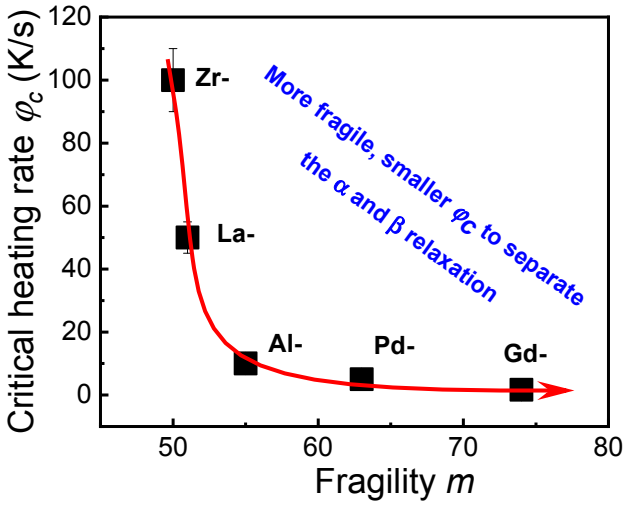

FIG. 6. Critical heating rate φ_C for separating the β relaxation from the α relaxation with fragility. The red arrowed curve gives the trend of φ_C with the increase of fragility m.

Table 1. Summary of data on the MG compositions and properties of the glass transition temperature T_g, the activation energy of α and β relaxation Q_α and Q_β by fitting the flash DSC data, the critical heating rate φ_C to separate the β relaxation from the α relaxation and the values

of fragility m from Ref. [53-55]. (The detailed calculations to confirm the fragility m for $La_{60}Ni_{15}Al_{25}$ and $Al_{88}Y_7Fe_5$ are seen in Fig. S3 [41].)

Compositions	T_g (K)	$Q_{\alpha\text{-}Kissinger}$ (kJ/mol)	$Q_{\alpha\text{-}Arrhenius}$ (kJ/mol)	$Q_{\beta\text{-}Kissinger}$ (kJ/mol)	$Q_{\beta\text{-}Arrhenius}$ (kJ/mol)	Q_β/Q_α	φ_C (K/s)	m
$Mg_{65}Cu_{25}Gd_{10}$	419	177±10.5	184±4.5	-	-	-	-	38
$Au_{49}Cu_{26.9}Ag_{5.5}Pd_{2.3}Si_{16.3}$	401	135±5	142±5	-	-	-	-	45
$Zr_{41.2}Ti_{13.8}Cu_{12.5}Ni_{10}Be_{22.5}$	618	552±20	564±24	106±7	113±7	0.192	100	50
$La_{60}Ni_{15}Al_{25}$	461	396±24	389±14	84.8±7	86±7	0.214	50	51
$Al_{88}Y_7Fe_5$	439	345±8	324±10	76.5±3	84±5	0.222	10	55
$Pd_{40}Ni_{10}Cu_{30}P_{20}$	560	426±13	417±14	97±4	95±6	0.228	5	63
$Gd_{55}Co_{25}Al_{20}$	590	438±15	448±14	104±4	104±5	0.237	1.67	74

controlled by tuning the kinetic fragility for MGs. Considering the relationship between the β relaxation and the mechanical properties and the diffusion behaviors [12-16], it will be very interesting to investigate the thermomechanical treatment, pre-loading and minor alloying effect on the relaxation behaviors and the related mechanical properties based on the Flash DSC with ultrafast heating rates, which is an ongoing study.

Based on the heat flow curves in Fig. 5, the effective activation energies for the β relaxation and the glass transition for all fragile MG systems were also calculated by fitting the Kissinger equation and the Arrhenius equation (the detailed calculations are in Fig. S3 [41]). First, for these fragile MGs, the Kissinger plots and the Arrhenius plots exhibit a linear relationship in the lower heating rate range, which is similar to that of Pd-based MG. These results indicate that the effective activation energies for β relaxation and glass transition can be roughly obtained. The detailed values of Q_β and Q_α are listed on the Table 1. It is evident that the values of Q_β and Q_α by the Kissinger and Arrhenius equations are also close. Thus, the following analyses and discussions about the values of Q_β and Q_α for different MGs are based on the values of the Kissinger equation fitting results. Second, for the β relaxations in the various MGs, there is a linear relationship between the Q_β and glass transition temperature T_g [15, 24]. Based on the above calculation results of Q_β and the corresponding glass transition temperatures, the ratio

between Q_β and RT_g can be calculated as shown in Fig. 7(a). The values of the ratio of Q_β and RT_g for all MG systems lie in the range of 21±3, which is consistent with the previous reports on the β relaxation of MGs [15, 24]. Moreover, to compare the effective activation energies of β relaxation and glass transition for various MGs, the values of the ratio of Q_β and Q_α for the above fragile MG systems are calculated and are included in the Table 1 as shown in Fig. 7(b). From Fig. 7(b), for the different MG systems, the ratio of Q_β and Q_α displays an ascending trend with the increase of the value of fragility. This result indicates that for the more fragile (larger m) glass formers, the difference between Q_β and Q_α is smaller. In the perspective of the potential energy landscape model for glasses, the activation of β relaxation should correspond to the jumping motion among the metastable energy states and the effective activation energy of β relaxation should be the energy difference of the bottom state and peak state of the current potential sub-basin [5]. The result in Fig. 7(b) indicates that the energy difference corresponding to the activation of β relaxation should become larger by taking the

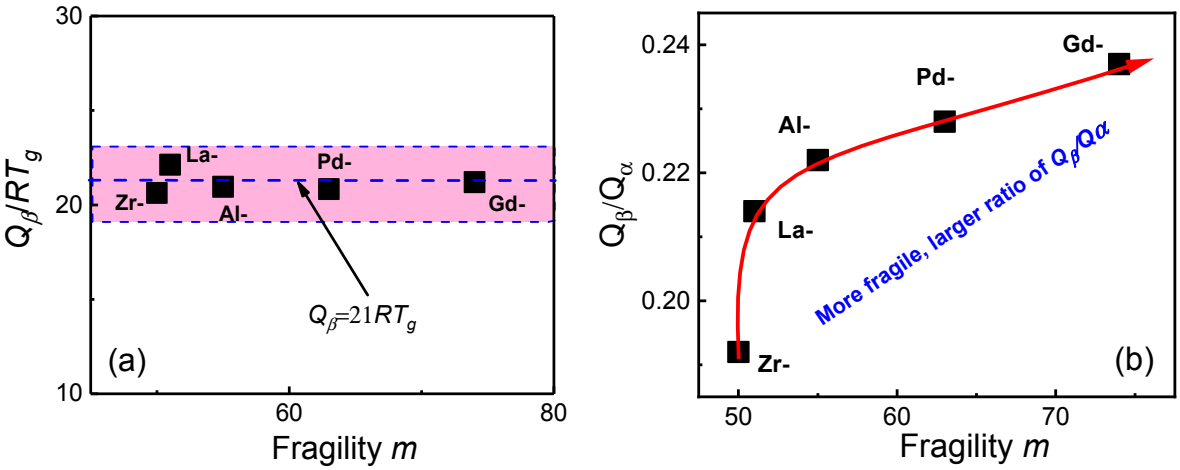

FIG. 7. (a) The ratio of Q_β/RT_g with the value of fragility m for different fragile MG systems. (b) The evolution of the effective activation energy ratio between Q_β and Q_a for the β relaxation and the glass transition (α relaxation) with fragility. The red arrowed curve gives the trend of the ratio value of the effective activation energies with the increase of fragility.

corresponding α relaxation activation energy as reference with the increase of the fragility. Thus, considering that the higher activation energy should accompany with a higher energy absorption,

the thermal signal of the endothermic reaction before the glass transition for more fragile MGs should be stronger than that of the less fragile MGs. Indeed, from the results in Fig. 2 and Fig. 5, with the increase of the heating rates, the thermal signal for the activation of β relaxation becomes stronger. Therefore, from this perspective, we can conclude that compared to the Pd MG, the β relaxations in less fragile MGs such as Al-, La- and Zr-based systems with small ratio of Q_β and Q_α can be only activated under larger heating rates, and the more fragile Gd-based MG with large ratio of Q_β and Q_α can activate the β relaxation under a lower heating rate.

C. Relaxation events under ultrafast heating in strong MGs

According to the potential landscape model, compared to the fragile glass formers, the strong glasses involve few single "metabasins" into which the cooling liquid could configurationally sample by surmounting barriers but encountering no substantial traps. Thus, the strong glasses display few relaxation events and usually exhibit the glass transition (α relaxation) [5, 52]. To investigate the relaxation behaviors for strong MGs under different heating rates, two strong glass

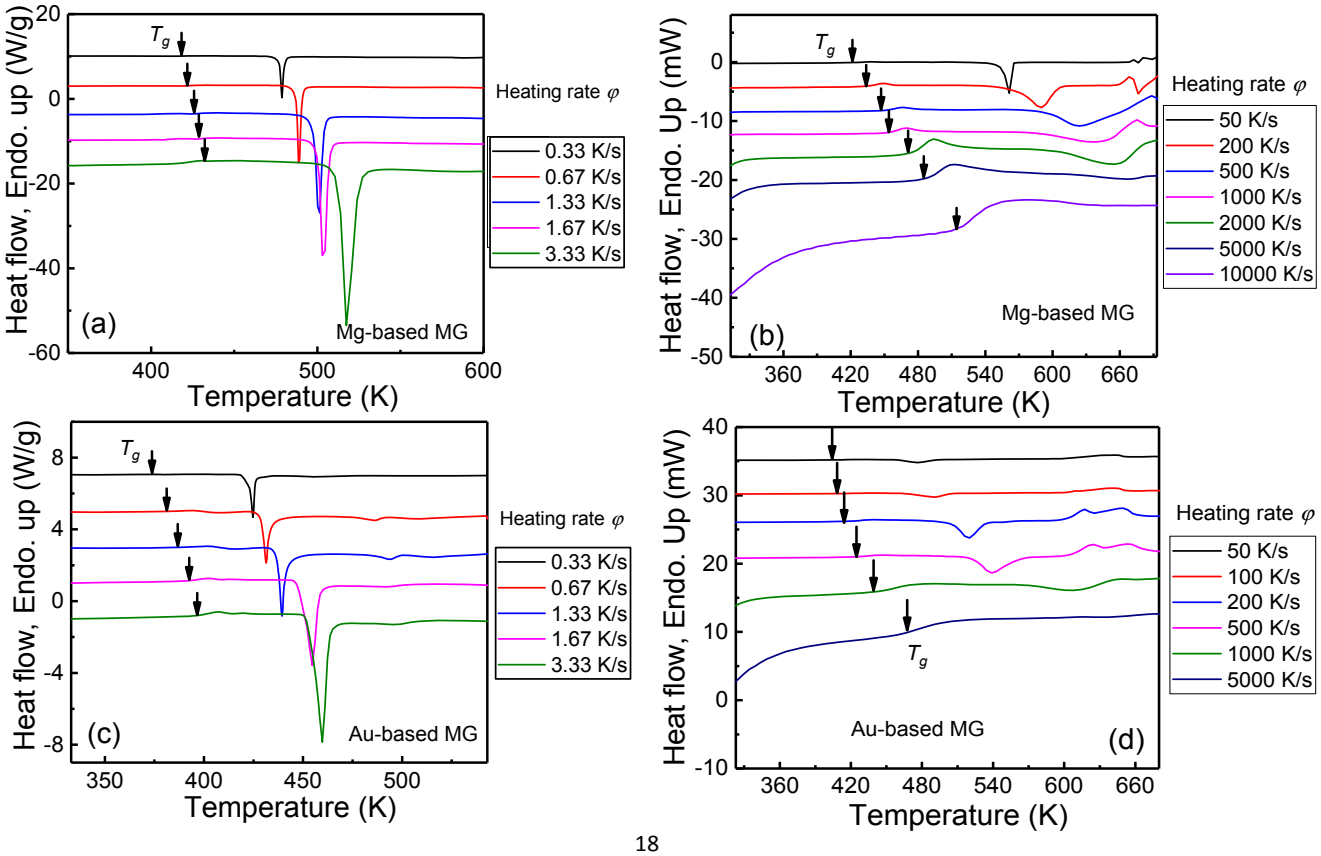

FIG. 8. A series of heat flow curves with different heating rates by Conventional DSC and Flash DSC for (a)-(b) $Mg_{65}Cu_{25}Gd_{10}$ and (c)-(d) $Au_{49}Cu_{26.9}Ag_{5.5}Pd_{2.3}Si_{16.3}$. The downward black arrows point to the glass transition temperatures.

formers: $Mg_{65}Cu_{25}Gd_{10}$ (m=38), $Au_{49}Cu_{26.9}Ag_{5.5}Pd_{2.3}Si_{16.3}$ (m=45) were selected. As shown in Fig. 8(a) - 8(d), a series of heat flow curves were measured by Flash DSC and conventional DSC for Mg- and Au-based MGs corresponding to different heating rates. Different from the obvious β relaxation signal before the glass transition for the fragile counterparts, the first endothermic reaction corresponding to β relaxation does not appear before glass transition for both of Mg- and Au-based MGs at different heating rates, which is consistent with the potential energy landscape model and the previous research about the β relaxation [53-54]. Moreover, the glass transition temperatures and the primary crystallization temperatures increase with the increase of heating rates for both of Mg- and Au-based MGs in Fig. 8(a) - 8(d). Based on these heat flow curves, the effective activation energy of α relaxation for strong MGs for Mg- and Au-based MGs can be calculated by fitting the Kissinger equation and Arrhenius equation at lower heating rate range and the detailed values are listed in Table 1. Based on the above evolution of the ratio of the effective activation energies for the β relaxation and the α relaxation with fragility in Fig. 7(b), the ratio of the effective activation energies for the β relaxation and the α relaxation is much smaller than those of the fragile MG counterparts. The results in Table 1 indicate that the effective activation energy of β relaxation may be much smaller than that of α relaxation in the strong MGs and the thermal signal of the activation of β relaxation seems much weaker than that of α relaxation. Thus, higher heating rates may be necessary to separate the β relaxation from α relaxation, which is not now available due to the current limited heating rate limit.

Meanwhile, two recent reports about high-speed heating kinetic viscosity measurements show that the kinetic viscosity for MGs decreases with an increase in heating rates and the strong MGs can display the similar kinetic behaviors of fragile glass formers at higher heating rates [59-60]. These findings imply that the higher heating rate can induce the strong-to-fragile transition and the strong glass formers will display the β relaxation under ultrafast heating rates that are beyond the capacity of the current Flash DSC. On the other hand, by further increasing the

heating rates via other methods (such as the capacitive discharge heating) [61], there should exist the possibility that can separate the β relaxation from the α relaxation in the strong MG systems.

D. Separation of β relaxation in fragile and strong glass formers via ultrafast heating

According to the framework of the potential energy landscape model, a glass-forming liquid system comprises a population of inherent states associated with local minima (basins) corresponding to the stable configurational states that are separated by saddle points or energy barriers [4-5]. The glass is supposed to locate at one of the local minima (or inherent states) in the potential energy landscape. A schematic description of the potential energy landscape models for fragile and strong glasses can be illustrated in the left parts of Fig. 9(a) and 9(b). Thus, based on two potential energy landscapes for fragile and strong glass formers, the β relaxation is considered to involve the stochastically and reversibly activated hopping events across "subbasins" confined within the inherent "megabasin" (intrabasin hopping) and the α relaxation is considered to involve the irreversible hopping events extending across different landscape megabasins (interbasin hopping). From this view, a potential nano-scale flow event, which is localized and confined by surrounding atoms, corresponds to the β relaxation activation; by contrast, the percolation of the flow units, entailing large scale atomic migration and irreversible structural change, leads to macroscopic yielding and plastic flow which corresponds to the α relaxation [18, 62]. For strong glasses, the potential energy landscape within the subbasins is considered to be more uniform than that for fragile glasses. Thus, it is understandable that the α and β relaxation bifurcation is weak or absent in the strong glasses. In contrast, the fragile glass formers exhibit significant cratering and distinct α andβ relaxation bifurcation [63]. Considering the difference of the kinetic behaviors for strong and fragile glasses, the scheme for the heterogeneous structure of strong and fragile MGs based on the simple flow unit model[55] can be shown in the middle parts of Fig. 9(a) and 9(b). For fragile MG systems, the difference between the flow unit regions and the elastic matrix is relatively large, and the flow unit regions have a much lower modulus, much lower viscosity and higher atomic mobility. Then, the difference of the kinetic characters between the flow unit regions and the elastic matrix is also large. Thus, under lower heating rates, the thermal signal of β relaxation originated from flow unit regions

can be easily separated from α relaxation. In contrast, the difference between the flow unit regions and the elastic matrix for strong glass formers is relatively small and the difference of the kinetic characters between the flow unit regions and the elastic matrix is also small. Thus, the critical heating rate to separate the β relaxation from the α relaxation for strong glass formers is much larger than that for fragile ones. For current experimental heating rate limit, the thermal signal for β relaxation cannot be obtained and there only appears the α relaxation. The detailed scheme of thermal activated relaxations for strong and fragile glasses is shown in the rights parts of Fig. 9(a) and 9(b).

Moreover, according to the above schematic description of the potential energy landscape models for fragile and strong glasses, the physical meaning of the critical heating rate to separate the β relaxation from α relaxation can be well understood. Based on our experimental results and the previous research of thermal β relaxation [26], the endothermic reaction during heating corresponds to the unfreezing of the local region fluctuations or the activation of the liquid-like flow units (in Fig. 9). When the heating rate range is lower than the critical cooling rate, the thermal signal corresponding to the activation of β relaxation is not strong enough to be detected by DSC and there is no endothermic peak in the heat flow curves. In contrast, when the heating rate range

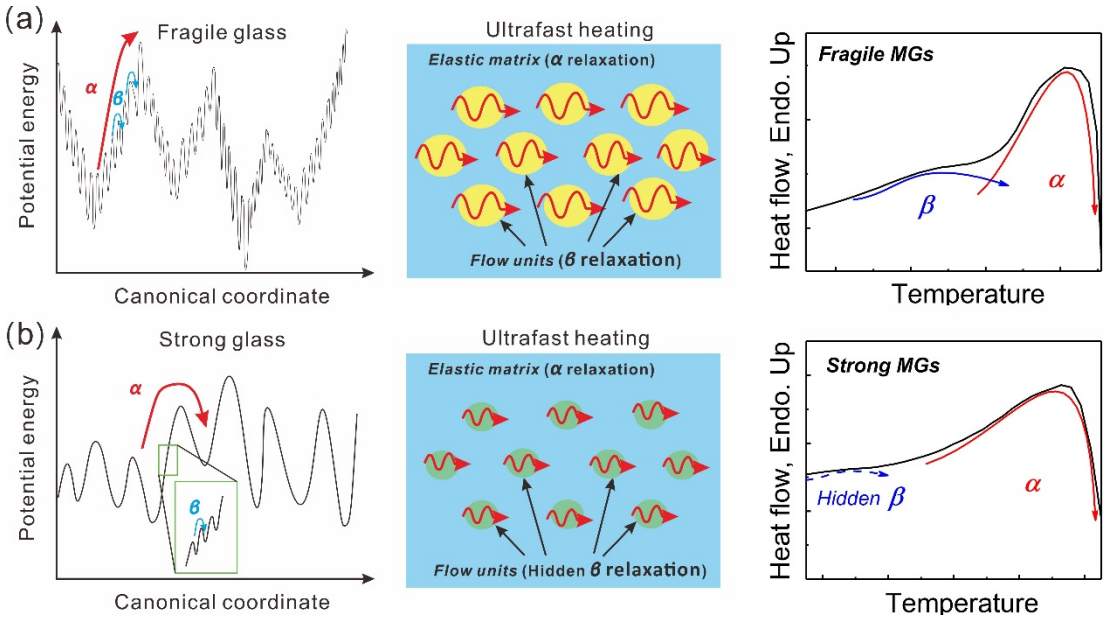

FIG. 9. (a) (Left) Potential energy landscape scheme for fragile glass systems. The red and blue arrows give the energy barrier transitions for β relaxation and α relaxation. (Middle) Flow unit

model for fragile glass systems and the activation for β relaxation under ultrafast heating. (Right) Scheme of the thermal signal of β relaxation and α relaxation for fragile glass systems. (b) (Left) Potential energy landscape scheme of strong glass systems. The red and blue arrows give the energy barrier transitions for β relaxation and α relaxation. (Middle) Flow unit model for strong glass systems and the activation for β relaxation under ultrafast heating. (Right) Scheme of the thermal signal of β relaxation and α relaxation for strong glass systems.

is larger than the critical heating rate, the thermal signal is high enough to be observed by DSC and is exhibited as an obvious endothermic peak in the heat flow curves. On the other hand, from the recovery enthalpy during heating, the e□ect of decrease in the enthalpy by structural relaxation during heating with heating rates below the critical value is very large and then the thermal signal from the β relaxation is relatively weak; when the e□ect of decrease in the enthalpy induced by the structural relaxation during heating with heating rates above the critical value is minimized, the thermal signal from the β relaxation becomes strong. Thus, the critical heating rate to separate the β relaxation from α relaxation is dependent on the microscopic heterogeneous structure of MGs [19-21]. From this perspective, when the microscopic structure is changed by structural relaxation or changing the composition, the critical heating rate should also change, which is on the way for our research.

It should be noted that there actually exist multiscale relaxation events in some MGs, such as the fast β relaxation and the γ relaxation [22, 64-65] and these secondary relaxations directly indicate that the potential energy landscape is more complex and even fractal [66]. It will be interesting to determine if additional secondary relaxation events can be activated by further increasing the heating rates in Flash DSC. Overall, the ultrafast heating method to separate the different relaxation events in this work provides a novel strategy to investigate the kinetic characters of multiscale relaxation events in amorphous materials.

IV. CONCLUSIONS

Based on a series of thermal analyses for several fragile and strong MG systems at different heating rates spanning over five orders of magnitude, a novel method was proposed to separate β relaxation from α relaxation via the ultrafast heating. For fragile MG systems, the obvious β

relaxation peak appears when the heating rate increases above a critical value; for strong systems, the β relaxation signal does not appear within the experimental heating rate limit. For the MG systems with increasing fragility, the critical heating rate to separate the β relaxation from α relaxation becomes smaller. Finally, based on the potential energy landscape model and the flow unit model of the heterogeneous structure for MGs, a pathway is proposed for the fragile and strong MGs to understand the physical mechanism for the separation of the β relaxation from the α relaxation via ultrafast heating. These results provide a new strategy based on the ultrafast Flash DSC platform to study the multiscale relaxation events in amorphous materials and the relationship with other physical properties, and offer an opportunity for an in-depth understanding of complex glass dynamics under different external stimuli.

ACKNOWLEDGEMENTS

M. Gao and J. H. Perepezko gratefully acknowledge the financial support from the Office of Naval Research (N00014-16-1-2401). Valuable discussions with W. Tang and experimental assistances from L. A. Turner, M. A. Nasr and A. M. Bossen are greatly appreciated.

REFERENCES

[1] G. P. Johari, M. Goldstei, Viscous Liquids and the Glass Transition. II. Secondary Relaxations in Glasses of Rigid Molecules, J. Chem. Phys. **53**, 2372 (1970).

[2] K. L. Ngai, Relaxation and Diffusion in Complex Systems. Springer. New York, 2011.

[3] M. D. Ediger, P. Harrowell, Perspective: Supercooled liquids and glasses, J. Chem. Phys. **137**, 080901 (2012).

[4] C. A. Angell, K. L. Ngai, G. B. McKenna, P. F. McMillan, S. W. Martin, Relaxation in glass forming liquids and amorphous solids, J. Appl. Phys. **88**, 3113 (2000).

[5] P. G. Debenedetti, F. H. Stillinger, Supercooled liquids and the glass transition, Nature **410**, 259 (2001).

[6] N. G. McCrum, B. E. Read, G. Williams, Anelastic and Dielectric Effects in Polymeric Solids. Wiley. New York, 1967.

[7] P. Hedwig, Dielectric Spectroscopy of Polymers. Wiley. New York, 1977.

[8] A. L. Greer, Metallic glasses…on the threshold, Mater. Today **12**, 14 (2009).

[9] C. A. Schuh, T. C. Hufnagel, U. Ramamurty, Mechanical behavior of amorphous alloys, Acta Mater. **55**, 4067 (2007).

[10] Z. F. Zhao, P. Wen, C. H. Shek, W. H. Wang, Measurements of slow β-relaxations in metallic glasses and supercooled liquids, Phys. Rev. B **75**, 174201 (2007).

[11] Z. Wang, H. B. Yu, P. Wen, H. Y. Bai, W. H. Wang, Pronounced slow β-relaxation in La-based bulk metallic glasses, J. Phys.: Condens. Matter **23**, 142202 (2011).

[12] H. B. Yu, W. H. Wang, K. Samwer, The β relaxation in metallic glasses: an overview, Mater. Today **16**, 183 (2013).

[13] H. B. Yu, X. Shen, Z. Wang, L. Gu, W. H. Wang, H. Y. Bai, Tensile Plasticity in Metallic Glasses with Pronounced β Relaxations, Phys. Rev. Lett. **108**, 015504 (2012).

[14] H. B. Yu, K. Samwer, Y. Wu, W. H. Wang, Correlation between β Relaxation and Self-Diffusion of the Smallest Constituting Atoms in Metallic Glasses, Phys. Rev. Lett. **109**, 095508 (2012).

[15] H. B. Yu, W. H. Wang, H. Y. Bai, Y. Wu, M. W. Chen, Relating activation of shear transformation zones to β relaxations in metallic glasses, Phys. Rev. B **81**, 220201(R) (2010).

[16] S. T. Liu, Z. Wang, H. L. Peng, H. B. Yu, W. H. Wang, The activation energy and volume of flow units of metallic glasses, Scr. Mater. **67**, 9 (2012).

[17] Y. H. Liu, T. Fujita, D. P. B. Aji, M. Matsuura, M. W. Chen, Structural origins of Johari-Goldstein relaxation in a metallic glass, Nat. Commun. 5 (2014) 3238.

[18] Z. Wang, B. A. Sun, H. Y. Bai, W. H. Wang, Evolution of hidden localized flow during glass-to-liquid transition in metallic glass, Nat. Commun. **5**, 5823 (2014).

[19] J. C. Ye, J. Lu, C. T. Liu, Q. Wang, Y. Yang, Atomistic free-volume zones and inelastic deformation of metallic glasses, Nat. Mater. **9**, 619 (2010).

[20] H. Wagner, D. Bedorf, S. Kuchemann, M. Schwabe, B. Zhang, W. Arnold, K. Samwer, Local elastic properties of a metallic glass, Nat. Mater. **10**, 439 (2011).

[21] T. Ichitsubo, E. Matsubara, T. Yamamoto, H. S. Chen, N. Nishiyama, J. Saida, K. Anazawa, Microstructure of Fragile Metallic Glasses Inferred from Ultrasound-Accelerated Crystallization in Pd-Based Metallic Glasses, Phys. Rev. Lett. **95**, 245501 (2005).

[22] Q. Wang, S.T. Zhang, Y. Yang, Y.D. Dong, C.T. Liu, J. Lu, Unusual fast secondary relaxation in metallic glass, Nat. Comm. **6**, 7876 (2015).

[23] J. C. Qiao, R. Casalini, Jean-Marc Pelletier, H. Kato, Characteristics of the Structural and Johari–Goldstein Relaxations in Pd-Based Metallic Glass-Forming Liquids, J. Phys. Chem. B **118**, 3720 (2014).

[24] L. N. Hu, Y. Z. Yue, Secondary Relaxation in Metallic Glass Formers: Its Correlation with the Genuine Johari−Goldstein Relaxation, J. Phys. Chem. C **113**, 15001 (2009).

[25] A. N. Tsyplakov, Y. P. Mitrofanov, A. S. Makarov, G. V. Afonin, and V. A. Khonik, Determination of the activation energy spectrum of structural relaxation in metallic glasses using calorimetric and shear modulus relaxation data, J. Appl. Phys. **116**, 123507 (2014).

[26] D. P. B. Aji, G. P. Johari, Kinetic-freezing and unfreezing of local-region fluctuations in a glass structure observed by heat capacity hysteresis, J. Chem. Phys. **142**, 214501 (2015).

[27] C. Zhou, Y. Z. Yue, L. N. Hu, Revealing the connection between the slow β relaxation and sub-Tg enthalpy relaxation in metallic glasses, J. Appl. Phys. **120**, 225110 (2016).

[28] E. Zhuravlev, C. Schick, Fast scanning power compensated differential scanning nano-calorimeter: 1. The device,Thermochim. Acta **505**, 1 (2010); E. Zhuravlev, C. Schick, Fast scanning power compensated differential scanning nano-calorimeter: 2. Heat capacity analysis,Thermochim. Acta **505**, 14 (2010).

[29] C. Schick, V. Mathot, Fast Scanning Calorimetry. Springer. Switzerland, 2016.

[30] H. E. Kissinger, Variation of peak temperature with heating rate in differential thermal analysis, J. Res. Natl. Bur. Stand. **57**, 217 (1956).

[31] T. V. Tropin, J. W. P. Schmelzer, C. Schick, On the dependence of the properties of glasses on cooling and heating rates: I. Entropy, entropy production, and glass transition temperature, J. Non-Cryst. Solids **357**, 1291 (2011).

[32] F. X. Bai, J. H. Yao, Y. X. Wang, J. Pan, Y. Li, Crystallization kinetics of an Au-based metallic glass upon ultrafast heating and cooling, Scr. Mater. **132**, 58 (2017).

[33] Jae-Chul Lee, Calorimetric study of β-relaxation in an amorphous alloy: An experimental technique for measuring the activation energy for shear transformation, Intermetallics **44**, 116 (2014).

[34] Y. X. Zhuang, W. H. Wang, Y. Zhang, M. X. Pan, D. Q. Zhao, Crystallization kinetics and glass transition of $Zr_{41}Ti_{14}Cu_{12.5}Ni_{10-x}Fe_xBe_{22.5}$ bulk metallic glasses, Appl. Phys. Lett. **75**, 2392 (1999)

[35] Z. Bian, A. Inoue, Ultra-Low Glass Transition Temperatures in Ce-Based Bulk Metallic Glasses, Mater. Trans. **46**, 1857 (2005).

[36] H. E. Kissinger, Reaction Kinetics in Differential Thermal Analysis, Anal. Chem. 29 (1957) 1702-1706.

[37] G. Ruitenberg, Applying Kissinger analysis to the glass transition peak in amorphous metals, Thermochim. Acta **404**, 207 (2003).

[38] Y. Shen, J. H. Perepezko, Investigation of the nucleation delay time in Al-based metallic glasses by high rate calorimetry, J. Non-Cryst. Solids **502**, 9 (2018).

[39] M. Gao, J. H. Perepezko, Flash DSC determination of the delay time for primary crystallization and minor alloying effect in marginal Al-based metallic glasses. Thermochimica Acta **677**, 91 (2019).

[40] B. Yang, J. W. P. Schmlelzer, B. G. Zhao, Y. L. Gao, C. Schick, Glass transition and primary crystallization of $Al_{86}Ni_6Y_{4.5}Co_2La_{1.5}$ metallic glass at heating rates spanning over six orders of magnitude, Scr. Mater. **162**, 146 (2019).

[41] See Supplemental Material at (URL) for the estimation of the cooling rate of the prepared amorphous ribbon-like samples, calculation of kinetic fragility for La- and Al-based metallic glasses, confirmation of the activation energy Q for β relaxation and α relaxation for Mg-, Au-, Zr-, La-, Al- and Gd-based metallic glass systems, calibration of the conventional DSC and Flash DSC instruments, and estimation of mass effect on the first endothermic reaction and glass transition for Pd-based metallic glass.

[42] X. H. Lin, W. L. Johnson, Formation of Ti–Zr–Cu–Ni bulk metallic glasses, J. Appl. Phys. **78**, 6514 (1995).

[43] W. H. Wang, The elastic properties, elastic models and elastic perspectives of metallic glasses, Prog. Mater. Sci. **57,** 487 (2012).

[44] G. V. Poel, D. Istrate, A. Magon, V. Mathot, Performance and calibration of the Flash DSC 1, a new, MEMS-based fast scanning calorimeter, J. Therm. Anal. Calorim. **110**, 1533 (2012).

[45] E. Shoifet, G. Schulz, C. Schick, Temperature modulated differential scanning calorimetry–extension to high and low frequencies, Thermochimica Acta **603**, 227 (2015).

[46] H. B. Ke, P. Wen, D. Q. Zhao, W. H. Wang, Correlation between dynamic flow and thermodynamic glass transition in metallic glasses, Appl. Phys. Lett. **96**, 251902 (2010).

[47] L. N. Hu, C. Zhou, C. Z. Zhang, Y. Z. Yue, Thermodynamic anomaly of the sub-Tg relaxation in hyperquenched metallic glasses, J. Chem. Phys. **138**, 174508 (2013).

[48] D. V. Louzguine-Luzgin, I. Seki, T. Yamamoto, H. Kawaji, C. Suryanarayana, A. Inoue, Double-stage glass transition in a metallic glass, Phys. Rev. B **81**, 144202 (2010).

[49] Y. Li, S. C. Ng, Z. P. Lu, Separation of glass transition and crystallization in metallic glasses by temperature-modulated differential scanning calorimetry, Phil. Mag. Lett. **78**, 213 (1998).

[50] L. S. Huo, J. F. Zeng, W. H. Wang, C. T. Liu, Y. Yang, The dependence of shear modulus on dynamic relaxation and evolution of local structural heterogeneity in a metallic glass, Acta Mater. **61**, 4329 (2013).

[51] I. Gallino, J. Schroers, R. Busch, Kinetic and thermodynamic studies of the fragility of bulk metallic glass forming liquids, J. Appl. Phys. **108**, 063501 (2010).

[52] C. A. Angell, Perspective on the glass transition, J. Phys. Chem. Solids **49** (1988) 863-871.

[53] J. C. Qiao, J. M. Pelletier, Q. Wang, W. Jiao, W. H. Wang, On calorimetric study of the fragility in bulk metallic glasses with low glass transition temperature:

(Ce0.72Cu0.28)90−xAl10Fex (x = 0, 5 or 10) and Zn38Mg12Ca32Yb18, Intermetallics **19**, 1367 (2011).

[54] G. Fiore, I. Ichim, L. Battezzati, Thermal analysis, fragility and viscosity of Au-based metallic glasses, J. Non-Cryst. Solids **356**, 2218 (2010).

[55] Z. Lu, W. H. Wang, H. Y. Bai, Classification of metallic glasses based on structural and dynamical heterogeneities by stress relaxation, Sci. China Mater. **6**, 98 (2015).

[56] C. A. Angell, Formation of Glasses from Liquids and Biopolymers, Science **267**, 1924 (1995).

[57] S. Mukherjee, J. Schroers, Z. Zhou, W. L. Johnson, W.-K. Rhim, Viscosity and specific volume of bulk metallic glass-forming alloys and their correlation with glass forming ability, Acta Mater. **52**, 3689 (2004).

[58] B. Zhang, R. J. Wang, D. Q. Zhao, M. X. Pan, W. H. Wang, Properties of Ce-based bulk metallic glass-forming alloys, Phys. Rev. B, **70**, 224208 (2004).

[59] T. Yamasaki, S. Maeda, Y. Yokoyama, D. Okai, T. Fukami, H. M. Kimura, A. Inoue, Viscosity measurements of Zr55Cu30Al10Ni5 supercooled liquid alloys by using penetration viscometer under high-speed heating conditions, Intermetallics, **14**, 1102 (2006).

[60] M. Zhang, Correlation between fragility and structural relaxation dynamics of bulk metallic glass-forming liquids, J. Chem. Phys. **551**, 164 (2013).

[61] W. L. Johnson, G. Kaltenboeck, M. D. Demetriou, J. P. Schramm, X. Liu, K. Samwer, C. P. Kim, D. C. Hofmann, Beating crystallization in glass-forming metals by millisecond heating and processing, Science **332**, 828 (2011).

[62] W. H. Wang, Y. Yang, T. G. Nieh, C. T. Liu, On the source of plastic flow in metallic glasses: Concepts and models, Intermetallics **67**, 81 (2015).

[63] F. H. Stillinger, A Topographic View of Supercooled Liquids and Glass Formation, Science **267**, 1935 (1995).

[64] L. Z. Zhao, R. J. Xue, Z. G. Zhu, K. L. Ngai, W. H. Wang, H. Y. Bai, A fast dynamic mode in rare earth based glasses, J. Chem. Phys. **144**, 204507 (2016).

[65] S. Kuchemann, R. Maaβ, Gamma relaxation in bulk metallic glasses, Scr. Mater. **137**, 5 (2017).

[66] P. Charbonneau, J. Kurchan, G. Parisi, P. Urbani, F. Zzamponi, Fractal free energy landscapes in structural glasses, Nat. Comm. **5**, 3725 (2014).